

# Evaluation of nuclear PGAM2 value in hepatocellular carcinoma prognosis

Yi-Ran Li<sup>a</sup>, Jin-Dong Chen<sup>b</sup>, Yu-Yao Zhu<sup>c</sup>, Ju-Tang Li<sup>d</sup>,  
Guang-Zhi Jin<sup>e</sup> and Ri-Ming Jin<sup>f</sup>

Phosphoglycerate mutase (PGAM) is a critical enzyme in glycolysis. PGAM2 is abundant in several types of tissues and malignant tumours. However, there is limited information regarding their clinicopathological significance in dysplastic nodules and hepatocellular carcinoma (HCC). This study aims to investigate the prognostic value of PGAM2 as a new biomarker for HCC. The PGAM2 expression level was evaluated by immunohistochemistry in liver cirrhosis ( $n = 10$ ), low-grade dysplastic nodules ( $n = 15$ ), high-grade dysplastic nodules ( $n = 15$ ) and HCCs ( $n = 20$ ) and 178 pairs of HCC and adjacent peritumoral liver tissues. We selected X-tile software for counting cut-point based on the outcomes for prognosis analysis, and used Kaplan–Meier analysis and Cox regression analysis can assess the prognosis of clinicopathologic parameters. Nuclear PGAM2 was significantly overexpressed in peritumoral liver tissues compared with HCC tissues ( $P = 0.0010$ ). Kaplan–Meier analyses of 178 HCC samples revealed that nuclear PGAM2's high expression level, but not cytoplasmic PGAM2, was significantly related to good overall survival rate (OS). In addition, univariate and multivariate Cox analyses indicated nuclear PGAM2 expression could be

regarded as valuable predictors for OS in HCC. PGAM2 was highly expressed in HCC tissues than liver cirrhosis tissues, and nuclear PGAM2's high expression might demonstrate HCC patients have poor postoperative results. Thus, nuclear PGAM2 can be regarded as valuable predictors for OS in HCC patients after surgery. *Anti-Cancer Drugs* 33: e500–e506 Copyright © 2021 The Author(s). Published by Wolters Kluwer Health, Inc.

*Anti-Cancer Drugs* 2022, 33:e500–e506

**Keywords:** formalin-fixed paraffin-embedded, hepatocellular carcinoma, immunohistochemistry, nuclear optical density, phosphoglycerate mutase

<sup>a</sup>Department of ICU, Eastern Hepatobiliary Surgery Hospital, <sup>b</sup>School of Basic Medical Sciences, <sup>c</sup>Department of Pathology, Eastern Hepatobiliary Surgery Hospital, Second Military Medical University, <sup>d</sup>Department of Gynecology and Obstetrics, <sup>e</sup>Department of Intervention, Tongren Hospital, Shanghai Jiao Tong University School of Medicine and <sup>f</sup>Department of First Surgery, Eastern Hepatobiliary Surgery Hospital, The Second Military Medical University, Shanghai, China

Correspondence to Ri-Ming Jin, MD, Department of First Surgery, Eastern Hepatobiliary Surgery Hospital, The Second Military Medical University, 225 Changhai Road, Shanghai 200082, China  
Tel: xx; e-mail: jinriming918@126.com

Received 14 May 2021 Revised form accepted 30 May 2021

## Introduction

Hepatocellular carcinoma (HCC) accounts for 90% of primary hepatic, it has become the modal type. HCC often occurs in patients with chronic hepatic diseases in China, like cirrhosis caused by HBV hepatitis or hepatitis C. People who consume excessive alcohol and accumulate fat in the liver also have a higher incidence of HCC. Treatment options include liver surgery, chemotherapy (either systemic or by hepatic artery infusion), immunotherapy, radiation therapy and others. Many HCC patients will have intermediate or advanced disease at the time of diagnosis [1]. It has been widely reported that China has a relatively high mortality rate compared with other countries [2].

Phosphoglycerate mutase (PGAM) catalyses the conversion of 3-phosphoglycerate (3-PGA) to 2-phosphoglycerate (2-PGA) in the glycolysis [3,4]. PGAM is a dimerise, which contains varying ratios of the fast-migrating brain isozyme (type B, PGAM1), slow-migrating muscle isoenzymes (type M, PGAM2) and hybrid form.

Previous clinical trials have suggested a possible relationship between PGAM2 and myocardial cells [5]. Li *et al.* used an HPLC-Chip-MS system to research the proteids when myocardial ischaemia occurred. In their samples, the PGAM2 level showed an increasing trend with longer ischaemic times. Among potential biomarkers of mild ischaemic myocardial injury, PGAM2 was more specific than others in cardiac tissues [6]. Research has also demonstrated that the constitutive overexpression of PGAM2 altered supersession of energy and decreased heart's antistress ability during heart failure [7].

PGAM upregulation has been identified as a common phenomenon in several cancers. A suggested mechanism for this reaction is as follows: Glucose oxidation is a chemical process that provides energy for normal

Supplemental Digital Content is available for this article. Direct URL citations appear in the printed text and are provided in the HTML and PDF versions of this article on the journal's website, [www.anti-cancerdrugs.com](http://www.anti-cancerdrugs.com).

This is an open-access article distributed under the terms of the Creative Commons Attribution-Non Commercial-No Derivatives License 4.0 (CCBY-NC-ND), where it is permissible to download and share the work provided it is properly cited. The work cannot be changed in any way or used commercially without permission from the journal.

cells to perform their required activities, whereas the primary mechanism of energy production for cancer cells is glycolysis. Upregulated glycolytic metabolism not only produces energy but also generates more biological intermediates, which maintain the cancer cells' proliferation, invasion, migration and metastasis. Some research showed that PGAM1 plays an important role in diverse cancers, including HCC, oral squamous cell carcinoma, clear cell renal cell carcinoma and colon and rectal carcinoma [8–12]. PGAM is upregulated in tumour cells in response to biological activity, and PGAM inhibition using small interfering RNAs or small molecules attenuates tumour growth and cell proliferation. Yan pin *et al.* reported that the acetylation mimetic mutant K100Q could substitute endogenous PGAM, which decreased NADPH production, restrained cell proliferation and tumour growth. Therefore, PGAM regulation and NADPH homeostasis play an important role in cell proliferation and tumour growth under oxidative stress conditions [13].

The protein expression of PGAM2 is significantly higher in cancer and glioma tissues, but the link between PGAM2 protein expression and HCC remains unclear. Regardless of the underlying cause, changes in gene expression play a key role in cancer cell development. Sarath *et al.* reported that gene set enrichment analysis revealed enhanced pathways specific to each stage, especially viral infection pathways in HCC initiation. Their research identified PGAM as a phase IV-specific gene, and the biomarkers they reported could be used as a supportive tool for the diagnosis and determination of optimal treatment targets in HCC [14]. Previous research has shown that PGAM expression in the nucleolus is a general phenomenon that occurs not only in neoplastically transformed cells but also in nonmalignant cells. The PGAM subunit is required for the nucleolar localization of PGAM, which is regulated by the insulin/IGF-1/PI3K signalling pathway and drugs inhibiting ribosomal biogenesis. They also proposed that PGAM silencing disrupted the nucleolar structure because PGAM interacted with several 40S and 60S ribosomal proteins, leading to inhibition of RNA synthesis and decreasing the mitotic index of squamous cell carcinoma cells [15]. The above results are consistent with the findings of this study that PGAM2 is highly expressed in the nucleus of HCC cells.

We determined the PGAM2 expression pattern in HCC tumour tissues and peritumoral tissues. PGAM2 was highly expressed in HCC than liver tissues around the tumour, and high expression of nuclear PGAM2 in HCC tissues might demonstrate HCC patients have poor post-operative results. Thus, nuclear PGAM2 can be seen as a prognostic biomarker for overall survival (OS) in HCC patients after surgery.

## Materials and methods

### Patients' samples

During January 2005 to December 2011, we stochastically collected 178 HCC formalin-fixed paraffin-embedded (FFPE) samples. These patients were treated at the Eastern Hepatobiliary Surgery Hospital (EHS). A total of 178 cases of tumour with peritumoral tissue were used as the expression pattern cohort. We maintained contact with patients for follow-up and observation until December 2014. This study got approved by the Institutional Review Committee (approval number: EHBHKEY2014-03-006) and informed consent in writing for all patients.

Sixty FFPE tissues of liver nodules were stochastically gathered retrospectively from sufferers who did radical resection from January 2005 to December 2011 in EHS (Supplementary Table, Supplemental digital content 1, <http://links.lww.com/ACD/A400> for clinicopathological features). Sixty tumour cases were analysed to identify differences in PGAM2 expression patterns between normal and diseased tissues of HCC patients, which included 10 cases of liver cirrhosis (LC), 15 cases of low-grade dysplastic nodules (LGDNs), 15 cases of high-grade dysplastic nodules (HGDNs) and 20 cases of HCCs.

The enrolment standard of HCC patients in this research were [16] (1) we considered the WHO histological diagnostic criteria as our diagnostic basis, (2) pathological diagnosis of hepatocytosis, (3) the patient did not receive anticancer therapy before surgery and had not occurred extrahepatic metastasis, (4) detailed follow-up data were obtained of 178 prognosis cohorts. OS was the interval between surgical operation to mortality or the final checking. The time-to-recurrence (TTR) meant time interval between tumour removal date until the neoplasm recurrence, mortality or final checking. After the first surgery year once every 3 months, patients had to accept follow-up. When until December 2014, they could conduct follow-up every 6 months. And we chose two physicians that not related to this research to conduct the follow-ups. Every patient about this research underwent abdominal ultrasound, X-ray for chest and serum alpha-fetoprotein (AFP) concentrations monitoring every one to 6 months in the first year after surgery, thereafter they conducted every three to six months. Every 6 months or suspected recurrence, we examined CT scanning or MRI of the abdomen. We strictly implement the same diagnostic criteria. We generated haematoxylin and eosin (HE) stained slides from FFPE tela. All samples were examined by two senior liver pathologists investigation [17].

### Tissue microarrays and immunohistochemistry

According to the reported approach to tissue microarray construction, immunohistochemistry and optical density (OD) measuring method [18,7]. Briefly, two veteran pathologists investigated and evaluated all HE-stained glass slides, prelabelled representative cores in the paraffin

blocks as well. Tissue cylinders with a diameter of 1.0 mm were dashed out of the labelled region, then merged into the receiving paraffin block. Then put the slices with thickness of 4- $\mu$ m on the glass slides dipped with 3-aminopropyltriethoxysilane. We implemented the method of dewaxing the paraffin sections in xylene and reducing the ethanol concentrations (one hundred percent, ninety-five percent and eighty-five percent, 5 min each time). We selected antigens, added citrate buffer of pH 6.0, irradiated them in the microwave for 3 min and with a room temperature cooling for 60 min. The slides were incubated in 3% H<sub>2</sub>O<sub>2</sub>/PBS to block endogenous peroxidase activity in addition goat serum was used to block nonspecific binding sites.

A rabbit polyclonal antibody we used against PGAM2 (507917; ZEN-BIOSCIENCE, China; 1:400 dilution, cytoplasmic and/or membrane staining) was the primary antibody. An EnVision Detection kit (GK500705; Gene Tech, Shanghai, China) made PGAM2 (human PGAM2 recombinant protein was used as an immunogen) directly visualization, and DAB served as the chromogenic agent. We reversed staining of tissue sections with haematoxylin for five minutes. All tests have established negative control slides without the primary antibody. The imaging system included a high-speed scanner connected to NanoZoomer S60 (Hamamatsu, Japan) was for OD measurement. Through high-speed scanning, specimens on glass slides could be transformed into high-resolution digital slice images. We counted and measured the ODs of each image by using the HALO software (Indica Lab, New Mexico, USA).

### Statistical analysis

We performed statistical analyses by using the SPSS statistical software package (SPSS Standard version 22.0; SPSS, Chicago, Illinois, USA) and Graph Pad Prism 8.01. We used X-tile software version 3.6.1 (Yale University School of Medicine, New Haven, Connecticut, USA) to obtain the most suitable critical point of PGAM2 expression for survival analysis [19]. Miller-Siegmund *P* value provides a corrected *P* value based on the model proposed by R Miller and D. Siegmund. This value is only displayed for two subpopulation cuts (e.g. *P* = 0.12 for X-tile be equal to *P* = 0.006 for SPSS). By means of Mantel-Cox logarithmic rank examine to evaluate the statistical significance of the correlation between PGAM2 expression and survival rate of patients. We carried on SPSS statistical software package (SPSS Standard version 22.0; SPSS) for correlation analysis between variables, single variable survival analysis, and multi-faced Cox proportional hazards regression. Two-tailed *P* value <0.05 was deemed to significant differences.

## Results

### Clinical features

One hundred and seventy-eight patients consisting of 18 women (10%) and 160 men (90%) with a median age

at diagnosis of 51.5 years were included in the expression pattern cohort. Clinical data and clinicopathological features of expression pattern cohort were shown in Table 1. Sixty patients, including 20 women (33%) and 40 men (67%) with the mean age at diagnosis of 58.8 years, were also included. Their clinical data and clinicopathological features were shown in Supplementary Table, Supplemental digital content 1, <http://links.lww.com/ACD/A400>.

### Features of PGAM2 expression in hepatocellular carcinoma tissues and peritumoral tissues

For the 178 HCC sufferers, X-tile software analysis was conducted to determine the optimal critical point of the nuclear OD value (NOD) and the cytoplasmic OD of PGAM2 expression. We used a standard logarithmic rank method to select a NOD of 0.42 and a cytoplasmic OD of 0.15 as the optimum critical point (Supplementary Figure 1, Supplemental digital content 1, <http://links.lww.com/ACD/A400>). Acquired from a lookup table for OS, the *P* value was statistically significant for the nuclear OD (*P* = 0.006), but the *P* value was not statistically significant for the cytoplasmic OD (*P* = 0.476) (Supplementary Figure 2,

**Table 1. Association of PGAM2 expression with clinicopathological features in 178 HCC patients**

Variable	PGAM2 NOD		<i>P</i> value
	Low	High	
Sex			0.029
	Men	119	41
	Women	9	9
Age			0.779
	≤50	61	25
	>50	67	25
HBs Ag			0.661
	Negative	22	10
	Positive	106	40
AFP			0.073
	Negative	46	11
	Positive	82	39
LC			0.220
	No	40	11
	Yes	88	39
TNM			0.530
	I	38	14
	II	73	26
	III	17	10
Child-Pugh			0.660
	A	115	46
	B	13	4
Tumour size			0.545
	≤5 cm	55	19
	>5 cm	73	31
Tumour number			0.481
	Single	101	37
	Multiple	27	13
Tumour differentiation			0.276
	Well	8	3
	Moderate	120	46
	Poor	0	1
Vascular invasion			0.962
	No	44	17
	Yes	84	33

AFP, a-fetoprotein; HBs Ag, hepatitis B surface antigen; HCC, hepatocellular carcinoma; LC, liver cirrhosis; NOD, nuclear optical density; TNM, tumour nodes metastases.

Supplemental digital content 1, <http://links.lww.com/ACD/A400>). Therefore, this study explored the relationship between the nuclear expression of PGAM2 and HCC.

PGAM2 staining of specimens showed nuclear immunoreactivity in HCC and peritumoral tissues (Fig. 1a,b). To compare the PGAM2 expression levels between HCC tumour tissues and peritumoral tissues in the expression pattern cohort (178 cases), OD values representing PGAM2 expression were inputted into GraphPad Prism software. As Fig. 1c,d showed, expression of PGAM2 in peritumoral tissues was slightly higher than HCC tissues ( $P < 0.05$ ).

#### Outcome-based cutoff point and Kaplan–Meier analysis

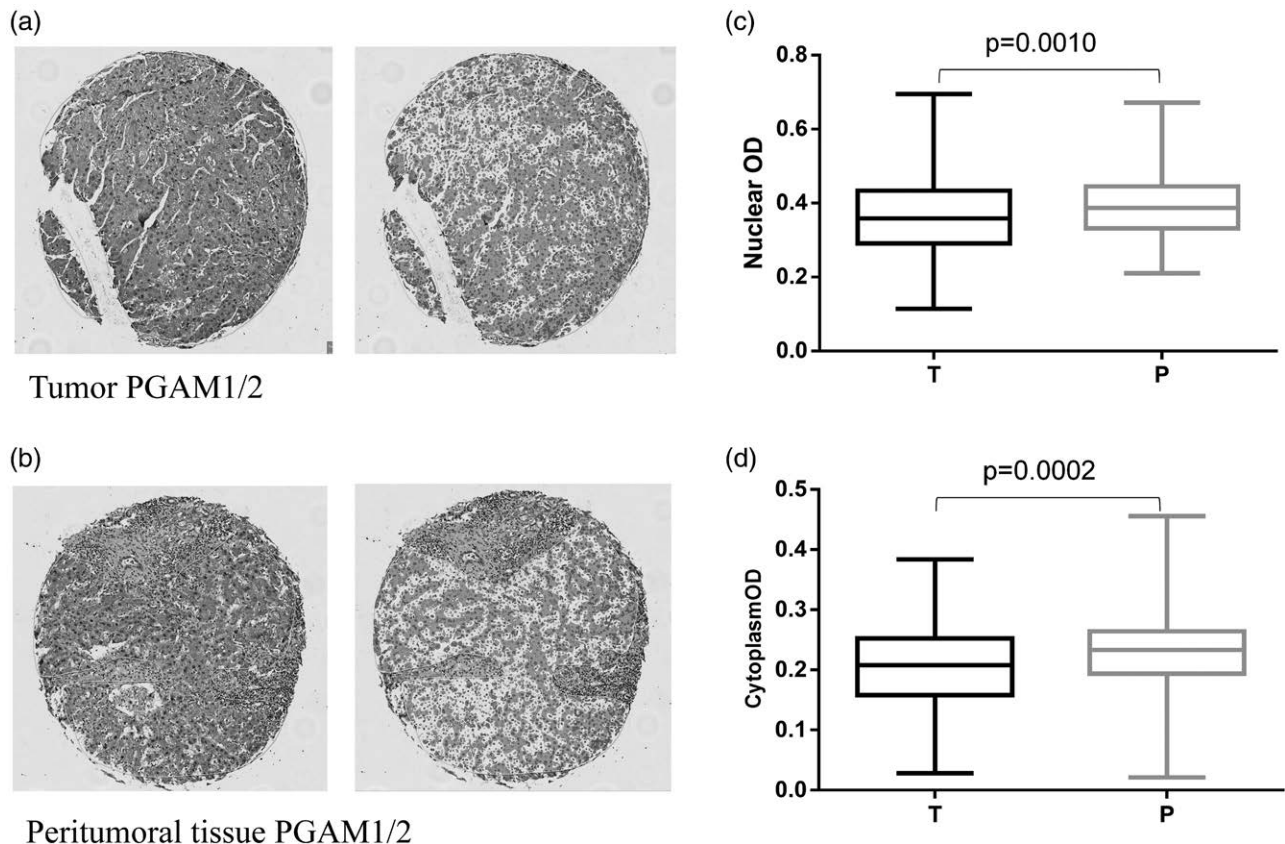
In order to gain the optimal critical point of PGAM2 expression for prognostic cohort survival analysis, we chose the X-tile program. The optimal critical points with minimum  $P$  values can be gained from OS lookup table (Supplementary Figure 1, Supplemental digital content 1, <http://links.lww.com/ACD/A400>), by using a standard logarithmic rank method.

As a result, the 178 HCC cases were assigned to two groups, with 128 cases in the low NOD group and 50

cases in the high NOD group. Then, SPSS 22.0 software was applied to describe curvilinear by Kaplan–Meier analysis.

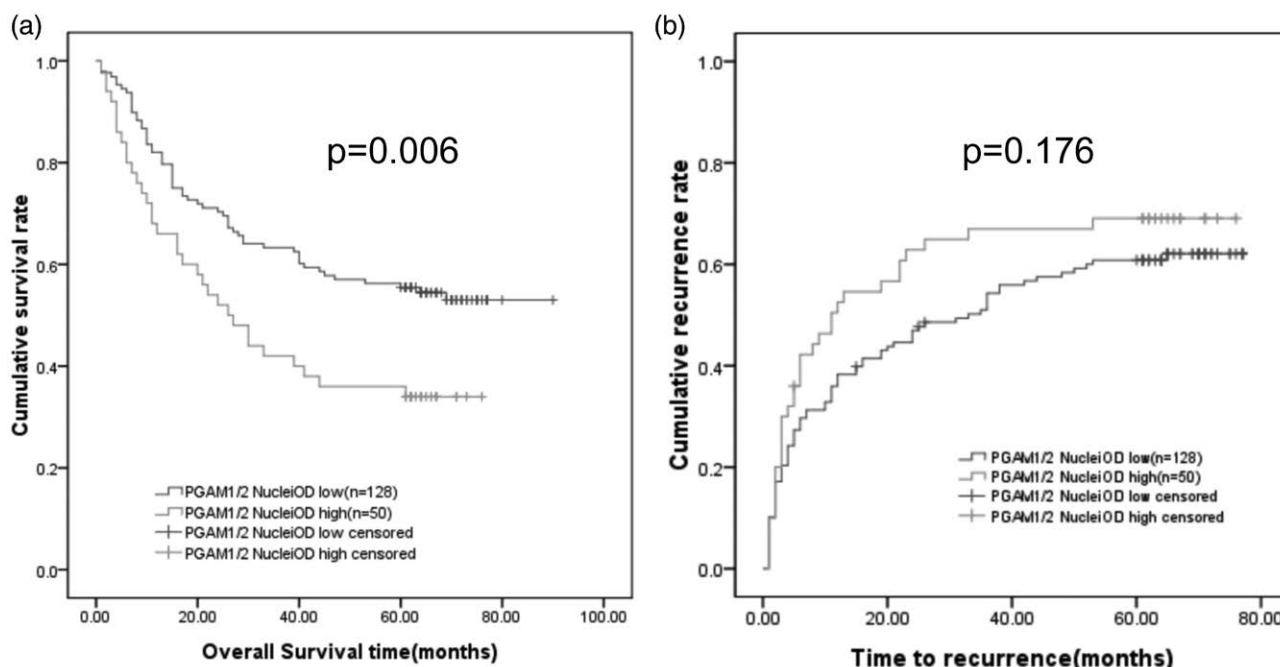
The outcomes indicated that the average OS time of HCC patients with low NOD PGAM2 values was 57.9 months, while the average time of HCC patients with high NOD PGAM2 values was 37.3 months ( $P = 0.006$ , logarithmic rank test; Fig. 2a). The average TTR for HCC patients with low NOD expression was 38.8 months, while that of HCC patients with high NOD expression was 30.2 months ( $P = 0.176$ , logarithmic rank test; Fig. 2b). The average OS time of HCC patients with low cytoplasm OD PGAM2 values was 43.4 months, while the average time of HCC patients with high NOD PGAM2 values was 54.5 months ( $P = 0.476$ , logarithmic rank test; Supplemental Figure 2A, Supplemental digital content 1, <http://links.lww.com/ACD/A400>). The average TTR for HCC patients with low cytoplasm OD expression was 31.5 months, while that of HCC patients with high cytoplasm OD expression was 37.6 months ( $P = 0.374$ , logarithmic rank test; Supplemental Figure 2B, Supplemental digital content 1, <http://links.lww.com/ACD/A400>).

Fig. 1



Immunohistochemical expression of PGAM2 in peritumoral tissues and paired HCC tissues. The expression characteristics of PGAM2 in (a) HCC tissue and (b) paired peritumoral tissue ( $\times 10$ ). (c,d) Box and whisker showing the average stain-strength of HCC tumour tissues (T) and paired peritumoral tissues (P) ( $P = 0.0010$  for NOD;  $P = 0.0002$  for cytoplasm OD). HCC, hepatocellular carcinoma; NOD, nuclear optical density.

Fig. 2



PGAM2’s Kaplan–Meier survival analyses in HCC sufferers. (a) The survival probability of HCC sufferers after surgery: low expression of PGAM2 NOD ( $n = 128$ , average value=57.9 months) and high expression of PGAM2 NOD ( $n = 50$ , average value=37.3 months). (b) Probability of recurrence for HCC patients after surgery: low expression of PGAM2 NOD ( $n = 128$ , average value=38.8 months) and high expression of PGAM2 NOD ( $n = 50$ , average value=30.2 months). HCC, hepatocellular carcinoma; NOD, nuclear optical density.

Table 2. Univariate and multivariate analyses of factors associated with OS in 178 HCC patients

Factors	Univariate <i>p</i>	OS		
		HR	95% CI	<i>P</i> value
Sex: men vs. women	0.511			
Age: ≤50 vs. >50	0.242			
HBs Ag: positive vs. negative	0.861			
AFP (ng/ml): ≤20 vs. >20	<b>&lt;0.0001</b>	2.829	1.591–5.068	<b>&lt;0.0001</b>
LC: yes vs. no	0.177			
TNM: I vs. II vs. III–IV	0.004			
Child–Pugh: A vs. B	0.228			
Tumour size: ≤5 vs. >5	<b>&lt;0.0001</b>	2.629	1.609–4.297	<b>&lt;0.0001</b>
Tumour number: single vs. multiple	<b>&lt;0.0001</b>	1.790	1.147–2.793	<b>0.010</b>
Tumour differentiation: well vs. moderate vs. poor	0.243			
Vascular invasion: no vs. yes	0.321			
PGAM1/2 NOD	<b>0.007</b>	1.647	1.070–2.535	<b>0.023</b>

Bold indicates significant difference in statistics.

AFP, a-fetoprotein; CI, confidence interval; HBs Ag, hepatitis B surface antigen; HCC, hepatocellular carcinoma; HR, hazard ratio; LC, liver cirrhosis; NOD, nuclear optical density.

### Association of PGAM2 expression with clinicopathological features of hepatocellular carcinoma patients

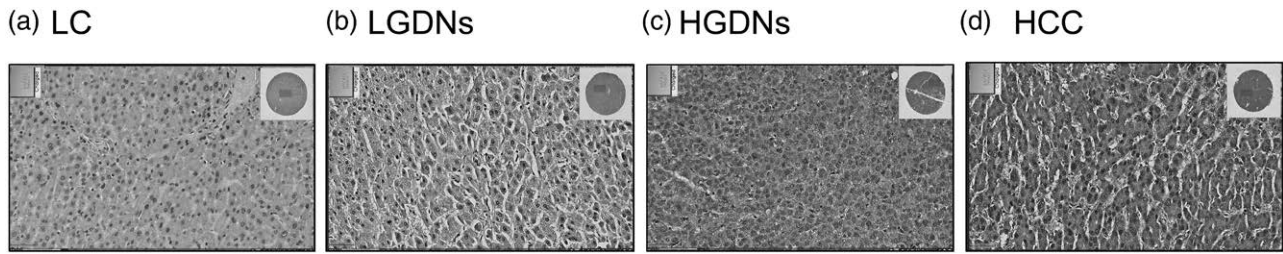
We discovered correlation between PGAM2 expression at the critical point based on outcome classification and clinical pathological factors in 178 HCC sufferers. We found PGAM2 expression was correlated with sex ( $P = 0.029$ ) but had nothing to do with others (Table 1).

### Univariate and multivariate survival analyses

Univariate analysis results indicated serum AFP, tumour size, tumour number and PGAM2 NOD were significantly correlated to OS ( $P$  values were <0.0001 for AFP, <0.0001 for tumour size, <0.0001 for tumour number and 0.007 for PGAM2 NOD) (Table 2).

Multivariate analysis adopts Cox multivariate proportional hazard regression model and is carried out gradually

Fig. 3



Immunohistochemical PGAM2 expression in LC, dysplastic nodules and HCC tissues. Expression characteristics of PGAM2 in LC tissue (a), LGDN tissue (b), HGDN tissue (c) and HCC tissue (d) ( $\times 10$ ). HCC, hepatocellular carcinoma; HGDN, high-grade dysplastic nodule; LC, liver cirrhosis; LGDN, low-grade dysplastic nodule.

(forward, conditional likelihood ratio). Univariate analysis significant factors included in the Cox multivariate proportional hazard regression analysis. The outcomes we gained indicated that serum AFP, tumour size, tumour number and PGAM2 NOD were OS's valuable factors of prognostic (Table 2).

#### Expression patterns of PGAM2 examined in liver cirrhosis, dysplastic nodules and hepatocellular carcinoma

We constructed four models for the independent verification set (LC = 10, LGDNs = 15, HGDNs = 15 and HCC = 20). Typical immunostaining of LC, dysplastic nodules and HCC was shown in Fig. 3. Similar to TMA analysis, PGAM2 was significantly upregulated compared among the four models. Notably, PGAM2 demonstrated high sensitivity for discriminating between HCC and LC.

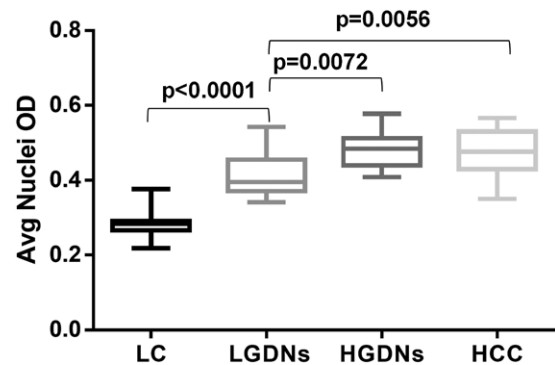
#### Association of PGAM2 expression with liver cirrhosis, low-grade dysplastic nodules, high-grade dysplastic nodules and hepatocellular carcinoma

In order to gain the comparison results that the expression levels of PGAM2 in 60 cases of LC tissues, precancerous lesions tissues and HCC tumour tissues, the NOD values representing PGAM2 expression were inputted into Graph Pad Prism software. As shown in Fig. 4, PGAM2 expression was frequently higher in LGDN tissues than LC ( $P < 0.0001$ ) and HGDN tissues compared with LGDN tissues ( $P = 0.0072$ ). In addition, PGAM2 levels were significantly higher in HCC tissues than in LGDN ( $P = 0.0056$ ), whereas no significant difference between HGDN tissues and HCC tumour tissues was observed ( $P = 0.9605$ ).

#### Discussion

HCC is one of the fatal cancers with a particularly poor prognosis in the world, and the liver is also a vulnerable part of cancer metastasis. Here, we identified a novel biomarker as an independent predictor of HCC's OS. Previous studies of PGAM have focused on the heart and skeletal muscle. The constitutive overexpression of PGAM modifies cardiac energy metabolism, which promotes heart failure because of the absence of cardiac

Fig. 4



The PGAM2 expression level in LC, LGDNs, HGDNs and HCC. A box diagram and whisker diagram of each model NOD was gained from the TMAs. Significant difference between HCC (20 pathological changes) and HGDNs (15 pathological changes) compared with LGDNs (15 pathological changes) displayed by the Mann-Whitney test. HCC, hepatocellular carcinoma; HGDNs, high-grade dysplastic nodules; LC, liver cirrhosis; LGDNs, low-grade dysplastic nodules; NOD, nuclear optical density.

stress resistance [7]. Early findings of PGAM may discover potential diagnostic and therapeutic biomarkers in terms of the pathology and biology of myocardial ischaemia [6]. PGAM2 is not detectable in liver tissues, but is highly expressed in the muscle and testis and moderately expressed in the heart and lung [7]. Lack of PGAM in humans can cause glycogen storage disease type X. Previous evidence showed PGAM deficiency in glycogen storage disease type X and novel mutations in the PGAM2 gene [20]. As a stage-IV-specific gene, PGAM2 RNA expression is found to be associated with HCC.

We evaluated the relevance of PGAM2 for HCC and found that their levels could accurately distinguish between HCC ( $n = 20$ ) and LC ( $n = 10$ ). Interestingly, PGAM2 expression gradually increased during disease progression, but no statistical differences between HGDN tissues and HCC tumour tissues were observed ( $P = 0.9605$ ), possibly due to a higher malignant potential of HGDN tissues. Therefore, PGAM2 was identified as a

predictive biomarker for HCC patients. We revealed that PGAM2 was overexpressed in HCC tissues. Our results provided evidence that nuclear PGAM2 expression was significantly higher in HCC tumour tissues compared with peritumoral tissues ( $P = 0.0010$  for NOD), as previously reported. PGAM2 localizes to nuclei and takes part in glycometabolism, and the PGAM2 gene plays an essential role in regulating muscle growth and development [3].

We demonstrated that determining the PGAM2 status using immunohistochemistry was a reliable strategy to assess HCC prognosis, but no statistical differences between PGAM2 expression and TTR was observed in HCC patients ( $P = 0.176$ ). As observed for nodal PGAM2, we demonstrated the prognostic value of OS for HCC patients. Our results also suggested that PGAM2 expression was not correlated to most clinical-pathological features in 178 HCC sufferers. As shown in Table 2, age is likely the only factor that is related to PGAM2 expression [10,21,22].

In a previous study, PGAM2 was found to be decreased in the soleus muscle of exercised rats following the pharmacological inhibition of Rho-kinase activity. Therefore, Rho-kinase signalling appears to be related to PGM2 expression [23]. Stable transfection of two PRMT4-site-specific (methyltransferase deficiency) mutants (CARM1/PRMT4 VLD and CARM1E267Q) significantly inhibits the PGAM2's expression. This provided a new method to decrease the level of PGAM2 [20]. Patients with primary muscle disorders are characterized by elevated levels of TNF- $\alpha$ , and TNF- $\alpha$  levels negatively affect the differentiation efficiency of muscle cell. In myoblast studies, it was found that the PGAM2 gene was regulated by TNF- $\alpha$  in independent myogenic differentiation studies. Therefore, in the early stages of HCC development, TNF- $\alpha$  may impact PGAM2 gene expression [24].

In conclusion, we demonstrate that nuclear PGAM2 is highly expressed in HCC than peritumoral tissues. We also demonstrate increasing nuclear PGAM2 levels could accurately classify our cases as LC or dysplastic nodules. High expression of nuclear PGAM2 in HCC tissues may determine that postoperative poor outcomes of HCC sufferers. Thus, nuclear PGAM2 is a valuable biomarker for OS in HCC sufferers after surgery. Our study might be helpful for clinicians to better understand the relationship between PGAM2 and HCC.

## Acknowledgements

This study was supported by the National Natural Science Foundation of China; 81972574 (G.-Z.J.).

Each patient or their guardians provided informed consent and the Ethics Committee of Eastern Hepatobiliary Surgery Hospital Research Ethics Committee approved the study.

## Conflicts of interest

There are no conflicts of interest.

## References

- Qin LX, Tang ZY. Recent progress in predictive biomarkers for metastatic recurrence of human hepatocellular carcinoma: a review of the literature. *J Cancer Res Clin Oncol* 2004; **130**:497–513.
- Yang T, Lu JH, Wu MC. Hepatocellular carcinoma in China. *BMJ (online)* 2010; **18**: c1026.
- Qiu H, Zhao S, Xu X, Yerle M, Liu B. Assignment and expression patterns of porcine muscle-specific isoform of phosphoglycerate mutase gene. *J Genet Genomics* 2008; **35**:257–260.
- Zhang J, Yu L, Fu Q, Gao J, Xie Y, Chen J, et al. Mouse phosphoglycerate mutase M and B isozymes: cDNA cloning, enzyme activity assay and mapping. *Gene* 2001; **264**:273–279.
- Wu Y, Chen S, Wen P, Wu M, Wu Y, Mai M, Huang J. PGAM1 deficiency ameliorates myocardial infarction remodeling by targeting TGF- $\beta$  via the suppression of inflammation, apoptosis and fibrosis. *Biochem Biophys Res Commun* 2021; **534**:933–940.
- Li H, Li J, Wang Y, Yang T. Proteomic analysis of effluents from perfused human heart for transplantation: identification of potential biomarkers for ischemic heart damage. *Proteome Sci* 2012; **10**:21.
- Okuda J, Niizuma S, Shioi T, Kato T, Inuzuka Y, Kawashima T, et al. Persistent overexpression of phosphoglycerate mutase, a glycolytic enzyme, modifies energy metabolism and reduces stress resistance of heart in mice. *Plos One* 2013; **8**:e72173.
- Li C, Shu F, Lei B, Lv D, Zhang S, Mao X. Expression of PGAM1 in renal clear cell carcinoma and its clinical significance. *Int J Clin Exp Pathol* 2015; **8**:9410–9415.
- Liu L, Wang S, Zhang Q, Ding Y. Identification of potential genes/proteins regulated by Tiam1 in colorectal cancer by microarray analysis and proteome analysis. *Cell Biol Int* 2008; **32**:1215–1222.
- Liu ZG, Ding J, Du C, Xu N, Wang EL, Li JY, et al. Phosphoglycerate mutase 1 is highly expressed in C6 glioma cells and human astrocytoma. *Oncol Lett* 2018; **15**:8935–8940.
- Ren F, Wu H, Lei Y, Zhang H, Liu R, Zhao Y, et al. Quantitative proteomics identification of phosphoglycerate mutase 1 as a novel therapeutic target in hepatocellular carcinoma. *Mol Cancer* 2010; **9**:81.
- Zhang D, Wu H, Zhang X, Ding X, Huang M, Geng M, et al. Phosphoglycerate mutase 1 predicts the poor prognosis of oral squamous cell carcinoma and is associated with cell migration. *J Cancer* 2017; **8**:1943–1951.
- Xu Y, Li F, Lv L, Li T, Zhou X, Deng CX, et al. Oxidative stress activates SIRT2 to deacetylate and stimulate phosphoglycerate mutase. *Cancer Res* 2014; **74**:3630–3642.
- Sarathi A, Palaniappan A. Novel significant stage-specific differentially expressed genes in hepatocellular carcinoma. *BMC Cancer* 2019; **19**:663.
- Gizak A, Grenda M, Mamczur P, Wisniewski J, Sucharski F, Silberring J, et al. Insulin/IGF1-PI3K-dependent nucleolar localization of a glycolytic enzyme—phosphoglycerate mutase 2, is necessary for proper structure of nucleolus and RNA synthesis. *Oncotarget* 2015; **6**:17237–17250.
- Chen KJ, Jin RM, Shi CC, Ge RL, Hu L, Zou QF, et al. The prognostic value of Niemann-Pick C1-like protein 1 and Niemann-Pick disease type C2 in hepatocellular carcinoma. *J Cancer* 2018; **9**:556–563.
- Tan N, Liu Q, Liu X, Gong Z, Zeng Y, Pan G, et al. Low expression of B-cell-associated protein 31 in human primary hepatocellular carcinoma correlates with poor prognosis. *Histopathology* 2016; **68**:221–229.
- Jin GZ, Li Y, Cong WM, Yu H, Dong H, Shu H, et al. iTRAQ-2DLC-ESI-MS/MS based identification of a new set of immunohistochemical biomarkers for classification of dysplastic nodules and small hepatocellular carcinoma. *J Proteome Res* 2011; **10**:3418–3428.
- Camp RL, Dolled-Filhart M, Rimm DL. X-tile: a new bio-informatics tool for biomarker assessment and outcome-based cut-point optimization. *Clin Cancer Res* 2004; **10**:7252–7259.
- Wang SC, Dowhan DH, Eriksson NA, Muscat GE. CARM1/PRMT4 is necessary for the glycogen gene expression programme in skeletal muscle cells. *Biochem J* 2012; **444**:323–331.
- Evans MJ, Saghatelian A, Sorensen EJ, Cravatt BF. Target discovery in small-molecule cell-based screens by in situ proteome reactivity profiling. *Nat Biotechnol* 2005; **23**:1303–1307.
- Li X, Tang S, Wang QQ, Leung EL, Jin H, Huang Y, et al. Identification of epigallocatechin-3-gallate as an inhibitor of phosphoglycerate mutase 1. *Front Pharmacol* 2017; **8**:325.
- Muoz VR, Gaspar RC, Esteca MV, Baptista IL, Vieira RFL, da Silva ASR, et al. Physical exercise increases ROCK activity in the skeletal muscle of middle-aged rats. *Mech Ageing Dev* 2020; **186**:111213.
- Meyer SU, Krebs S, Thirion C, Blum H, Krause S, Pfaffl MW. Tumor necrosis factor alpha and insulin-like growth factor 1 induced modifications of the gene expression kinetics of differentiating skeletal muscle cells. *PLoS One* 2015; **10**:e0139520.